A Role for N-Myristoylation in Protein Targeting: NADH-Cytochrome b_5 Reductase Requires Myristic Acid for Association with Outer Mitochondrial But Not ER Membranes

Nica Borgese,*‡ Diego Aggujaro,* Paola Carrera,§ Grazia Pietrini,* and Monique Bassetti*

*Consiglio Nazionale delle Ricerche Cellular and Molecular Pharmacology Center, Department of Pharmacology, University of Milan, 20129 Milan, Italy; ‡Faculty of Pharmacy, University of Reggio Calabria, 88021 Roccelletta di Borgia, Catanzaro, Italy; and §Scientific Institute "San Raffaele," 20132 Milan, Italy

Abstract. N-myristoylation is a cotranslational modification involved in protein–protein interactions as well as in anchoring polypeptides to phospholipid bilayers; however, its role in targeting proteins to specific subcellular compartments has not been clearly defined. The mammalian myristoylated flavoenzyme NADH-cytochrome b_5 reductase is integrated into ER and mitochondrial outer membranes via an anchor containing a stretch of 14 uncharged amino acids downstream to the NH_2-terminal myristoylated glycine. Since previous studies suggested that the anchoring function could be adequately carried out by the 14 uncharged residues, we investigated a possible role for myristic acid in reductase targeting. The wild type (wt) and a nonmyristoylatable reductase mutant (gly2→ala) were stably expressed in MDCK cells, and their localization was investigated by immunofluorescence, immuno-EM, and cell fractionation. By all three techniques, the wt protein localized to ER and mitochondria, while the nonmyristoylated mutant was found only on ER membranes. Pulse-chase experiments indicated that this altered steady state distribution was due to the mutant's inability to target to mitochondria, and not to its enhanced instability in that location. Both wt and mutant reductase were resistant to Na_2CO_3 extraction and partitioned into the detergent phase after treatment of a membrane fraction with Triton X-114, demonstrating that myristic acid is not required for tight anchoring of reductase to membranes. Our results indicate that myristoylated reductase localizes to ER and mitochondria by different mechanisms, and reveal a novel role for myristic acid in protein targeting.

N-MYRISTOYLATION, which consists in the cotranslational attachment of the 14 carbon saturated fatty acid, myristic acid, via an amide bond, to the NH_2-terminal glycine of target proteins, is a highly specific modification required for the function of a number of regulatory proteins and enzymes. The myristoylating enzyme(s) is located in the cytosol and transfers the myristoyl moiety from myristoyl–coenzyme A to the NH_2 terminus of acceptor nascent chains, provided that their first five residues conform to a loose consensus sequence in which the NH_2-terminal glycine (gly2) is essential. With one exception, N-myristoylation has been found to be a constitutive and irreversible modification (for reviews see Johnson et al., 1994; Casey, 1995).

Studies on a variety of N-myristoylated proteins suggest that myristic acid may have different roles when attached to different acceptor proteins. Its most obvious and simple function is that of contributing to the association of the modified protein to the cytosolic face of membranes. However, myristic acid alone is not sufficient to anchor a protein to the phospholipid bilayer, as indicated both by binding studies on model peptides (Peitzsch and McLaughlin, 1993) and by the existence of soluble myristoylated proteins, such as calcineurin B (Aitken et al., 1982; Zhu et al., 1995) and the catalytic subunit of cAMP-dependent protein kinase (Carr et al., 1982). More sophisticated roles for myristic acid include: (*a*) participation in a "switch" mechanism permitting the protein to cycle in a regulated manner between membranes and the cytosol (McLaughlin and Aderem, 1995; Randazzo et al., 1995; Zozulya and Stryer, 1992; Tanaka et al., 1995); (*b*) influencing protein conformation, with consequences for protein stability (Yonemoto et al., 1993) or ligand binding (Franco et al., 1995; Randazzo et al., 1995; Ames et al., 1995; and (*c*) promotion of protein–protein interactions (Linder et al., 1991; Harris and Neil, 1994).

As a result of its demonstrated role in protein–protein interactions, it seems possible that myristic acid, in addition to participating in the anchoring of proteins to the phospholipid bilayer, might play a role in the selection of the target membrane to which the myristoylated protein binds, i.e., in protein targeting. However, since different

Address all correspondence to Nica Borgese, C.N.R. Cellular and Molecular Pharmacology Center, via Vanvitelli 32, 20129 Milan, Italy. Tel.: (39) 2-70146250. Fax: (39) 2-7490574. e-mail: Nica@Farma1.csfic.mi.cnr.it

myristoylated proteins are associated with different membranes, it is clear that myristic acid by itself cannot constitute a targeting signal. Rather, it could be part of a more complex signal, or, by influencing protein conformation, it could be instrumental in the display of a signal located elsewhere on the protein molecule. Until now, it has been difficult to discriminate experimentally between an anchoring and a targeting role for myristic acid. This is because the membrane-associated myristoylated proteins that have been investigated require the fatty acid for anchorage, and the corresponding nonmyristyolated mutants are relocated to the cytosol (Cross et al., 1984; Graff et al., 1989; Jones et al., 1990; Mumby et al., 1990; Yu and Felsted, 1992; Busconi and Michel, 1993; D'Souza-Schorey and Stahl, 1995).

An N-myristoylated protein that might allow the experimental distinction between a targeting and anchoring role for myristic acid is mammalian NADH-cytochrome (cyt)[1] b_5 reductase (generally referred to in this paper simply as "reductase") (Ozols et al., 1984). This protein inserts posttranslationally into ER and mitochondrial outer membranes (MOMs) (Borgese and Pietrini, 1986; Borgese et al., 1980; Borgese and Gaetani, 1980) via an NH_2-terminal anchor, which is myristoylated in both these locations (Borgese and Longhi, 1990). The COOH-terminal catalytic domain is exposed to the cytosol (for review see Borgese et al., 1993). The NH_2-terminal anchoring sequence contains, in addition to myristic acid, a stretch of 14 uncharged amino acids, which, on the basis of fluorescence quantum yield studies on a tryptophan residue contained therein, appears to interact directly with the interior of the lipid bilayer (Kensil and Strittmatter, 1986). In vitro binding studies have shown that myristic acid is not required for the interaction of reductase with liposomes (Strittmatter et al., 1993), suggesting that the 14 uncharged residues are sufficient for anchoring and that the myristic acid may play a more subtle role, possibly in the selection of the target membrane. In the present study, we have tested this hypothesis by comparing the localization of a nonmyristoylatable G2A mutant with that of the wild-type reductase in transfected cultured mammalian cells. We find that indeed the mutant protein, while remaining membrane bound, has a dramatically altered subcellular distribution, in that it no longer localizes to mitochondria but retains its capacity to bind to ER membranes.

Materials and Methods

Plasmid Constructions

DNA manipulations were carried out by standard procedures (Sambrook et al., 1989; Ausubel et al., 1987). Two cDNAs, coding for the rat wild-type myristoylated and for a G2A nonmyristoylatable form of reductase, were used in this study and are referred to as "wt" and "G2A" cDNA, respectively (see Fig. 1). Wild-type (wt) cDNA in the plasmid pGEM3 (corresponding to the construct pGbk3 described in Pietrini et al., 1992) was used as template for the construction of the G2A mutant by PCR-assisted mutagenesis. The upper mutagenic primer, corresponding to nucleotides (nts) 25–47 of the sequence in Pietrini et al., (1988), was: 5′ TTCGCCACCATGGCGGCCCAGCT 3′ (underlined sequence is NcoI restriction site, containing the start codon; boldfaced C is the substituted base, generating the G2A mutation); the lower primer, spanning nts 142–122 of the sequence in Pietrini et al. (1988), was: 5′ CTTGATGTCGGGGTTCTCGAG 3′ (underlined sequence is unique XhoI restriction site of reductase cDNA). After purification and digestion with XhoI and NcoI, the 112-bp PCR-generated fragment was used to replace the corresponding fragment in the wt cDNA. The absence of unwanted substitutions in the mutant clone, as a result of the amplification process, was checked by sequencing.

For expression in mammalian cells, wt and G2A cDNA were subcloned into the vector pCB6 (Brewer and Roth, 1991), in which the KpnI–BamHI fragment of the polylinker was replaced with the corresponding fragment of pBluescript II SK. wt cDNA was excised from pGEM3 with KpnI upstream of the cDNA, within the polylinker, and BalI in the 3′ untranslated region (position 953), and cloned into the KpnI and EcoRV sites of the modified pCB6 to generate pCB6wt. G2A cDNA was excised from pGEM3 with KpnI and cloned into the KpnI site of the modified pCB6 to generate pCB6G2A.

A plasmid coding for a fusion protein containing the first 11 residues of the gene 10 protein of phage T7 attached to the entire rat reductase sequence was constructed by inserting a filled 998 NcoI–NdeI fragment of wt cDNA into the filled BamHI site of of the pET3a vector (Novagen, Madison, WI), generating the plasmid pET3a.wt.

Antibodies

Most of the immunofluorescence and immunoblotting experiments were performed with an anti-rat reductase antibody raised in a rabbit, using the bacterially expressed fusion protein encoded in pET3a.wt as immunogen. Inclusion bodies, containing the expressed fusion protein, were collected by sedimentation, solubilized with 0.1% SDS, emulsified in Freund's complete adjuvant, and injected into a rabbit subcutaneously at multiple sites on the back. The resulting antiserum was affinity purified on a strip of nitrocellulose containing the electrophoretically purified fusion protein (Olmsted, 1981).

For double immunofluorescence labeling of reductase together with organelle marker antigens for which rabbit polyclonal antibodies were available, a goat antiserum against the hydrophilic catalytic fragment of the enzyme purified from rat liver (Meldolesi et al., 1980) was used. For immunoprecipitation, an antiserum raised in rabbit against the hydrophilic fragment of the enzyme was used.

Other antibodies used in this study were: (*a*) a polyclonal antiserum, against bovine complex III, provided by R. Bisson (University of Padova, Italy); complex III was purified according to Yu et al., (1974) and antibodies were raised as described by Vaitukaitis (1981). The antibodies recognized all of the polypeptides of the complex and were not cross-reactive with cytochrome oxidase polypeptides; (*b*) an anti-rat ER antibody (Louvard et al., 1982), provided by D. Louvard (Curie Institute, Paris, France); (*c*) an affinity-purified anti-dog ribophorin I polyclonal antibody (Nicchitta et al., 1991), obtained from G. Migliaccio (Istituto di Ricerche di Biologia Molecolare, Rome, Italy); (*d*) an mAb against protein disulfide isomerase (PDI) from StressGen (Victoria, British Columbia, Canada).

Secondary FITC-labeled anti-rabbit IgG raised in donkey were from Jackson Immunoresearch Laboratories, Inc. (West Grove, PA). Biotinlyated monoclonal anti-goat IgG and Texas red–conjugated streptavidin were from Sigma Chemical Co. (St. Louis, MO) and Amersham Intl. (Little Chalfont, UK), respectively. Goat anti-mouse and anti-rabbit IgG, conjugated to 5- and 10-nm gold particles, respectively, were from British Biocell Intl. (Cardiff, UK).

Biochemical Assays

Reduced and alkylated samples were analyzed by SDS-PAGE and blotted onto nitrocellulose as described (Borgese and Pietrini, 1986). Samples were routinely analyzed on 11% gels; however, for blotting of ribophorin, 7% gels were sometimes used. Immunostaining of blots was carried out either by the enhanced chemiluminescence (ECL) procedure, using reagents from Amersham Intl. according to the instructions of the manufacturer, or with ^{125}I-protein A (200,000 dpm/ml; Amersham Intl.) as secondary reagent, followed by autoradiography, as previously described (Borgese and Pietrini, 1986). For quantitative analysis of radioimmunoblotting experiments, autoradiograms were scanned with a laser densitometer (Ultrascan XL; LKB Instruments, Inc., Gaithersburg, MD). Alternatively, radioactive bands were excised from the nitrocellulose and counted in an auto-gamma-counter (Cobra; Packard Instrument Co., Inc., Down-

1. *Abbreviations used in this paper*: cyt, cytochrome; ECL, enhanced chemiluminescence; HMR, heavy microsomal fraction; MOM, mitochondrial outer membrane; MR, microsomal fraction; PDI, protein disulfide isomerase; SRP, signal recognition particle; wt, wild type.

ers Grove, IL). Different dilutions of the antigens to be assayed were always analyzed to be sure that the assay was linear.

Protein was assayed by the method of Lowry (Lowry et al., 1951). NADH-$[Fe(CN)_6]^{3-}$ reductase and NADH-cyt c reductase were assayed as described in previous publications (Borgese and Pietrini, 1986; Shirabe et al., 1995).

Transfection and Selection of Cell Lines Stably Expressing Reductase Forms

MDCK II cells were grown in MEM with Earl's salts, supplemented with 10% FCS, 2 mM L-glutamine, 100 U/ml penicillin, 100 mg/ml streptomycin, 10 mg/ml gentamicin, and maintained at 37°C under a 5% CO_2 atmosphere. Cells grown on a plastic substrate to ~50% confluence were transfected by the calcium phosphate method (Graham and Van der Eb, 1973), using 1 μg of Qiagen-purified plasmid per cm^2 of monolayer. Cells were incubated at 37°C for 6–9 h with the DNA precipitate in the presence of 0.1 mM chloroquine diphosphate (Sigma Chemical Co.). After removal of the DNA-containing medium, the cells were subjected to a glycerol shock (MEM minus FCS containing 15% glycerol for 5 min at room temperature) (Parker and Stark, 1979). Transfected cell lines were selected by growth in the antibiotic G418 (0.9 mg/ml) (GIBCO BRL, Gaithersburg, MD). Resistant colonies were expanded in 24-well petri dishes. After reaching confluency, monolayers were washed free of medium and analyzed by SDS-PAGE followed by immunoblotting. Reductase-expressing clones were further purified by limiting dilution. Stably transfected cell lines were maintained in culture in medium supplemented with 0.5 mg/ml G418.

Immunofluorescence and Immunogold-EM

Cells plated on 1.7 × 1.7 cm^2 glass coverslips were grown to 50% confluency, and then fixed with 4% paraformaldehyde in 0.120 M sodium phosphate buffer, pH 7.4, for 30 min at 37°C. The monolayers were permeabilized and processed for immunofluorescence as described (De Silvestris et al., 1995). Preparations were observed using a microscope (Axioplan; Zeiss, Oberkochen, Germany) equipped for epifluorescence.

For immunogold-EM, cells plated on 10-cm petri dishes were detached by trypsinization, collected by centrifugation, and fixed for 30 min on ice with 4% paraformaldehyde and 0.2% glutaraldehyde in 0.1 M sodium phosphate buffer, pH 7.3. Cell pellets were equilibrated in concentrated sucrose, frozen, sectioned, incubated with antibodies, postfixed, stained, and embedded as previously described (Bassetti et al., 1995). The sections were first incubated with anti-PDI mAbs, used as a marker for the ER, followed by anti-mouse IgG–10-nm gold particle conjugates, and then with anti-reductase antibodies followed by anti-rabbit IgG–5-nm gold particle conjugates. Stained sections were observed and photographed with a CM10 electron microscope (Philips Electronic Instruments, Inc., Mahwah, NJ).

To quantitate the results obtained with the immunogold technique, fields containing areas of ER and mitochondria were photographed at a magnification of 21,000 and printed with further 2.5-fold enlargement. Density of gold particles in cytoplasmic areas not containing mitochondria was determined using a calibrated grid, composed of 0.25 × 0.25-μm cells, randomly placed over the prints. Grid cells (0.0625 μm^2 areas) that contained zero or one 10-nm gold particles were classified as PDI negative, while those containing two or more were classified as PDI (ER) positive. 5-nm gold particles (reductase) were counted in both PDI-positive and -negative areas. The average density of gold particles in PDI-positive and -negative areas for each micrograph was calcuated from the total number of particles counted in each of the two areas, divided by the total PDI-positive or -negative area (number of grid cells × 0.0625 μm^2) examined. Density of gold particles over mitochondria was estimated within areas delimited by a contour line traced at a distance of ~12 nm from the margin of the mitochondrial profiles. The linear density was determined by counting particles that fell within 12 nm on either side of the outer membrane. Mitochondrial areas and contour lengths were measured with the NIH Image program, after generating electronic versions of the prints.

Cell Fractionation

Cells grown to ~70% confluence on 175-cm^2 petri dishes were washed free of medium with PBS containing 5 mM EDTA (PBS-EDTA), scraped from the dishes with a rubber policeman, and recovered by centrifugation (130 *g* for 10 min). After resuspension in 2 ml homogenization buffer (0.25 M sucrose, 0.1 mM EDTA, 20 mM Tris-HCl, pH 7.4, 1 mM PMSF, 0.5 μg/ml leupeptin, 0.7 μg/ml pepstatin, 2 μg/ml aprotinin), cells were again sedimented at 325 *g* for 7 min in a refrigerated microfuge. Cells were then incubated for 5 min on ice in 0.75 ml of hypotonic buffer (20 mM Tris HCl, pH 7.4, 0.1 mM EDTA, 15 mM KCl). After addition of an equal volume of 2 × concentrated homogenization buffer, cells were ruptured by 10 passages through a cell cracker with a 0.0007-inch clearance. The homogenate was centrifuged at 780 *g* for 10 min to sediment nuclei. The nuclear pellet was resuspended in 1 ml of homogenization buffer, and then recentrifuged as above. The two supernatants were combined and centrifuged again as above, and the resulting postnuclear supernatant, containing 60–70% of the protein of the total homogenate, was centrifuged at 9,300 *g* for 10 min to sediment mitochondria. The mitochondrial pellet was washed twice by resuspension in 0.4 M sucrose containing the same ions and protease inhibitors as the homogenization buffer, and centrifugation was performed at 6,000 *g* for 10 min. The postmitochondrial supernatant was centrifuged at 15,000 *g* for 10 min to obtain a heavy microsomal fraction (HMR). The resulting supernatant was centrifuged for 45 min at 150,000 *g* in the TLA-100.3 rotor (Beckman Instruments, Inc., Palo Alto, CA) to obtain a microsomal pellet (MR) and a high speed supernatant. Pellets were resuspended in a small volume of homogenization buffer.

Immunoprecipitation

Suspensions containing metabolically labeled cells or cell fractions were lysed with an equal volume of lysis buffer (50 mM Tris-Cl, pH 7.5, 20 mM EDTA, 0.3 M NaCl, 4% Triton X-100, 2 mM PMSF, 1 μg/ml leupeptin, 1.4 μg/ml pepstatin, 4 μg/ml aprotinin) for 10 min on ice. Lysates were depleted of nuclei by centrifugation at 800 *g* for 10 min, and then supplemented with methionine, cysteine, and gelatin to final concentrations of 0.5 mM, 0.25 mM, and 0.25%, respectively. After clarification by centrifugation (12,0000 *g*, 10 min), the lysates were incubated overnight at 4°C with anti-reductase antiserum at 1:50 dilution. Protein A–Sepharose Cl-4B beads (Pharmacia, Uppsala, Sweden) in excess of the serum IgG were added, and the samples were incubated in a multivortex for 1 h in the cold room. Protein A beads were collected by low speed centrifugation and washed twice with TBS containing 0.5% Triton X-100 and once with the same buffer without detergent. The beads were then heated in SDS solubilization buffer, and the released, reduced proteins were alkylated and analyzed by SDS-PAGE. Immunoprecipitated reductase was detected by fluorography (Bonner and Laskey, 1974) or by autoradiography of a blot of the gel.

Metabolic Labeling and Pulse-Chase Experiments

Before labeling with ^3H-myristic acid (16 Ci/mmol from Dupont-New England Nuclear, Wilmington, DE), ~70% confluent cells were incubated for 45 min in medium containing dialyzed and delipidated (Cham and Knowles, 1976) FCS. This medium was replaced with fresh medium containing similarly treated FCS, to which the tritiated fatty acid, dissolved in a small volume of DMSO, was added to a final concentration of 335 μCi/ml. Cells were incubated with the tritiated fatty acid for 6 h, and then processed for immunoprecipitation and fluorography.

Before labeling with ^{35}S-amino acids, cells grown to ~70% confluence were incubated for 45 min in medium lacking methionine and cysteine and containing dialyzed FCS. The cells were then incubated in the same medium, but containing ^{35}S-translabel (ICN Pharmaceuticals, Costa Mesa, CA) at concentrations and for the times specified in the figure legends. In pulse-chase experiments, after the incubation with radioactive amino acids, monolayers were chilled, washed free of radioactive medium, and then returned to the incubator with complete medium. Mitochondrial and heavy microsomal fractions were prepared from cells arrested at the different chase times and subjected to immunoprecipitation with anti-reductase antibodies. The immunoprecipitates were analyzed by SDS-PAGE followed by blotting. An evaluation of the ratio of metabolically labeled reductase molecules to total reductase molecules in the immunoprecipitates ("metabolic specific radioactivity") was obtained as follows: the blots, which contained all the immunoprecipitates from one experiment, were first directly exposed to x-ray film. The ^{35}S-content of the bands was quantitated by scanning the developed films with an LKB Ultroscan XL laser densitometer. The total amount of reductase (^{35}S-labeled plus unlabeled) in the bands was then evaluated by radioimmunoblotting. Bound ^{125}I–protein A was determined by cutting out the bands and counting them in a γ-counter. The ratio of ^{35}S (area from scanning) to ^{125}I counts was taken as a measure of the metabolic specific radioactivity. Since the

absolute value of this ratio varied in different experiments, as a function of time of exposure of the unprocessed blots and of the specific radioactivity of the ^{125}I–protein A, for each experiment, the ratio for each fraction and each time point was normalized to the average ratio obtained in both cell fractions at all time points.

Treatment of Membranes with Na_2CO_3 or Triton X-114

A postnuclear supernatant (see Materials and Methods [Cell fractionation]), prepared from cells expressing wt or G2A reductase, was centrifuged at 150,000 *g* for 45 min in the TLA-100.3 rotor to obtain a total membrane pellet. The pellet was resuspended in a small volume of homogenization buffer. 100-μl aliquots containing 150 μg of protein were supplemented with an equal volume of 0.2 M Na_2CO_3, pH 11.2, incubated on ice for 30 min, and then centrifuged at 60,000 rpm for 1 h in the TLA-100 rotor. Pellets were resuspended with 0.1 M Na_2CO_3 to the same final volume as the supernatants. Equal aliquots of pellets and supernatants were analyzed by SDS-PAGE followed by ECL immunoblotting.

Aliquots of membrane suspensions (30–100 μg protein) were treated with Triton X-114 in a total volume of 150 μl as described by Bordier (1981). Equal aliquots of aqueous and detergent phases were analyzed by SDS-PAGE followed by ECL immunoblotting.

Results

Expression of wt and G2A Reductase in MDCK Cells

Cyt b_5 reductase is anchored to the phospholipid bilayer via an NH_2-terminal anchor containing a stretch of 14 uncharged amino acids (*underlined* in Fig. 1) preceded by the consensus sequence for myristoylation (*boldfaced* in Fig. 1), which results in myristoylation of Gly in position 2 (*boxed* in Fig. 1) after removal of the initiator Met. To investigate the role of myristic acid in the localization of reductase, we constructed a mutant in which Gly2 was changed to Ala (G2A mutant). MDCK cells were transfected with cDNAs coding for the wt or mutant reductase, and G418-resistant clones, stably expressing the reductase forms, were selected. The results presented in this paper were all obtained with a single clone for each reductase form, referred to respectively as wt- and G2A-MDCK; however, at least three independent clones for each construct, as well as transiently transfected CV1 cells, were analyzed by immunofluorescence and yielded indistinguishable results.

To compare the expression of the transfected reductase forms in our cell lines with that of endogenous reductase and to directly assess the lack of myristyolation of the mutant, we incubated the transfected and control MDCK cells either with ^{35}S-labeled amino acids or ^{3}H-myristic acid, and then analyzed immunoprecipitates from the labeled cells by SDS-PAGE fluorography. As shown in Fig. 2, the labeling pattern of total proteins of control and transfected cells was indistinguishable (lanes *1–3*). In contrast, detectable ^{35}S-labeled reductase polypeptide was not immunoprecipitated from control cells (lane *4*), while a prominent band at the expected position was visible in immunoprecipitates from both wt and G2A reductase cells (lanes *5* and *6*). When ^{3}H-myristic acid was used as labeling agent, only immunoprecipitates from cells expressing wt reductase contained a radioactive polypeptide (lane *8*), demonstrating that the G2A mutant was not myristoylated (lane *9*), as expected. This experiment also showed that reductase endogenous to MDCK cells was expressed at sufficiently low levels to not interfere with the analysis of the transfected enzyme forms.

Although the G2A mutation is at the extremity of the NH_2-terminal anchoring domain of the reductase, it was possible that it had an indirect effect on the conformation of the catalytic domain, resulting in the production of nonnative, possibly aggregated enzyme. To investigate this point, the transfected cell lines were analyzed for reductase enzyme activity (Table I). Two different enzyme assays specific for reductase, the NADH-cyt c and the NADH-$[Fe(CN)_6]^{3-}$ reductase assays, were used. With the NADH-cyt c reductase assay, wt and G2A-expressing cells showed 4.2- and sevenfold more activity, respectively, than control cells (Table I, *second column*). The increase in activity was more pronounced with the NADH-$[Fe(CN)_6]^{3-}$ reductase assay (5.4- and 11.7-fold over control cells for wt and G2A cells, respectively; *fourth column*). The lower increase observed with the first assay may be due to its dependency on endogenous membrane-bound cyt b_5, which serves as intermediate electron carrier and is present at very low concentrations in MDCK cells (our unpublished observations). The higher activity of the G2A-MDCK relative to wt cells could in large part be explained by their higher reductase protein content, as is apparent from the data of the third and fifth columns, in which the reductase activity in the homogenates is normalized to reductase content, determined by radioimmunoblotting. The data, normalized in this way, reflect the turnover number of the enzyme and are similar for the two reductase forms, although the value for the mutant enzyme remained slightly higher. The results indicate in any case that the G2A mutation did not lead to loss of function of the catalytic domain, in agreement with previous data on the bacterially expressed enzyme (Strittmatter et al., 1993).

1 17 24
Met Gly Ala Gln Leu Ser Thr Leu Ser Arg Val Val Leu Ser Pro Val Trp Phe Val Tyr Ser Leu Phe *Met Lys*.....

Figure 1. Membrane anchor of rat NADH-cyt b_5 reductase. The NH_2-terminal 25 residues are shown. The residues in boldface constitute the consensus sequence for myristoylation. Met in position 1 is removed by an aminopeptidase, and gly2 is then myristoylated. The 14 underlined residues constitute a hydrophobic stretch that interacts with the phospholipid bilayer (see text). Met 24 (*italics*) is the last residue of the hydrophobic stretch, which is followed by the COOH-terminal 275-residue, cytosolically exposed, catalytic domain. Met 24 also is the start codon of the soluble form of reductase, expressed in erythrocyte precursors from an alternate transcript (Pietrini et al., 1992).

Table I. Reductase Activity in Total Homogenates of Control (Nontransfected), wt, and G2A MDCK

Cell line	NADH-cyt c reductase		NADH-$[Fe(CN)_6]^{3-}$ reductase	
	*nmol/min/ mg protein**	*nmol/min/ cpm × 10^{6}‡*	*nmol/min/ mg protein**	*nmol/min/ dpm × 10^{6}‡*
Control	46.9	ND	786	ND
Wt	199.6	41.7	4,256	889
G2A	328.3	50.8	9,170	1,420

*Activity normalized to total protein in the homogenates.
‡Activity normalized to reductase antigen quantitated by ^{125}I–protein A radioimmunoblotting (dpm in bands excised from blots; see Materials and Methods).

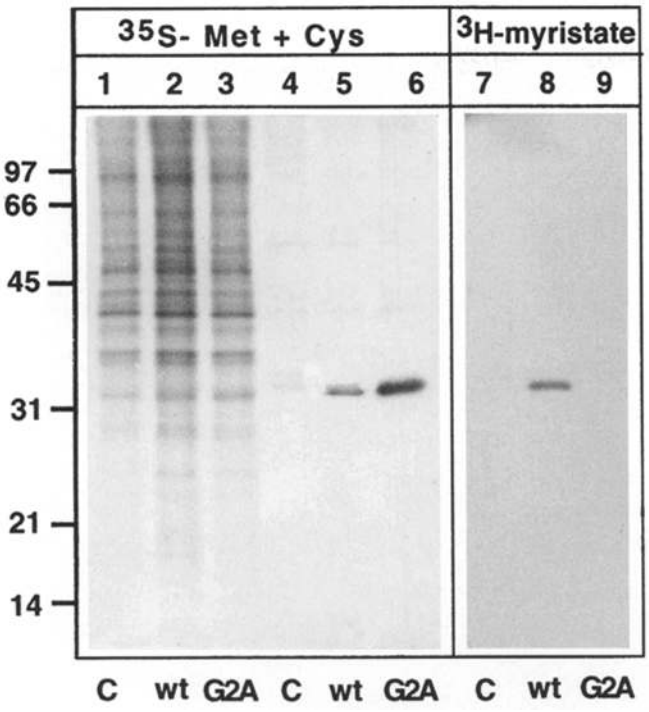

Figure 2. SDS-PAGE analysis of wt and G2A reductase expressed in transfected MDCK cells shows lack of myristoylation of G2A mutant. Control (*C*, lanes *1*, *4*, and *7*), wt (lanes *2*, *5*, and *8*), or G2A (lanes *3*, *6*, and *9*) MDCK cells, grown to ~70% confluency in 10-cm petri dishes, were incubated with either 0.1 mCi/ml ^{35}S-labeled methionine + cysteine for 90 min (lanes *1–6*) or 0.335 mCi/ml ^{3}H-myristic acid for 6 h. Cell lysates were prepared in total volumes of 1 ml, and reductase was immunoprecipitated. Samples were analyzed by 11% SDS-PAGE followed by fluorography. (Lanes *1–3*) ^{35}S-labeled proteins of total lysates (1 μl); (lanes *4–6*) immunoprecipitates obtained from 100 μl ^{35}S-labeled lysates; (lanes *7–9*) immunoprecipitates obtained from 200 μl ^{3}H-myristic acid–labeled lysates. Lanes *1–6* and *7–9* were exposed overnight and for 5 d, respectively. Numbers on the left represent $M_r \times 10^{-3}$ of molecular weight standards from Bio Rad Laboratories (Richmond, CA).

Different Localization of wt and G2A Reductase Assessed by Immunofluorescence and Immuno-EM

From biochemical studies, it has been known for a long time that, in liver, reductase is localized to the MOM and to ER membranes (Borgese and Pietrini, 1986; Meldolesi et al., 1980; Sottocasa et al., 1967), and that in both its locations it is myristoylated (Borgese and Longhi, 1990). As demonstrated in Figs. 3, 4, and 7 *A*, also in transfected cultured cells, the product of wt reductase cDNA showed the same double localization previously found for the endogenous enzyme in liver.

When wt-MDCK cells were stained with an anti-reductase antibody, a punctate pattern superimposed on a more diffuse reticular staining was observed (Figs. 3 *A* and 4 *A*). We consistently observed that not all cells were positive for reductase (Fig. 3, *asterisks*). Since our cells belonged to a single clone, we presume that this heterogeneity may be attributed to temporal alterations in the level of expression of the transfected cDNA as a result of changes in the metabolic state of the cells. Fig. 3 shows the results of an experiment in which cells were doubly immunostained for reductase (*A*) and for complex III, as a marker for mitochondria (*B*). The punctate portion of the anti-reductase antibody staining corresponded closely to the pattern obtained with the anti–complex III antibody. The arrowheads in *A* and *B* highlight some of the points of coincident staining. However, the more reticular, diffuse staining obtained with the anti-reductase antibody was not seen with the anti–complex III antibody. Moreover, anti-reductase clearly stained the nuclear envelope (*A*, *arrow*), indicating the presence of wt reductase on the ER. The presence of wt reductase on the ER was confirmed by a double immunostaining experiment with anti-reductase and an antibody directed against ER membrane proteins (Louvard et al., 1982) (Fig. 4), from which the coincidence of the reductase reticular staining and the ER pattern was evident (compare Fig. 4 *A* and 4 *B*).

Having characterized the immunofluorescence pattern for wt reductase, we next analyzed the cells expressing the mutant G2A reductase (Figs. 5 and 6). As can be seen in Fig. 5 *A*, the mutant reductase did not localize to the discrete structures positive for the wt enzyme (Fig. 5 *B*) and shown to be mitochondria. Rather, it showed exclusively a diffuse reticular staining. Double staining with the anti-reductase and the anti-ER antibodies revealed a high degree of coincidence between the two patterns (Fig. 6). These results thus suggest that the nonmyristoylated reductase is capable of associating with the ER but has lost its capacity to bind to the MOM.

To confirm these results at the ultrastructural level, ultrathin cryosections were analyzed in double-labeling experiments with the immunogold technique, using anti-PDI antibodies to identify the ER. As shown in Fig. 7 *A*, wt reductase (small gold particles) was present both on mitochondria and on PDI-positive structures (large gold). The Golgi complex (*G*) was negative both for wt-reductase and for PDI. Small gold particles were present at the periphery of the mitochondria, as shown in the inset of Fig. 7 *A*, consistent with the MOM localization of reductase. Some apparently more internal labeling might be attributable to a tangential orientation of the section plane. However, we cannot rule out that a part of wt reductase has an inverted topology, with the catalytic domain facing the intermembrane space. In contrast with the situation with wt-reductase, mitochondria of G2A-expressing cells were labeled poorly or not at all, as illustrated in Fig. 7 *B*, although localization on PDI-positive structures was evident (Fig. 7 *B*, *arrows* and *inset*).

The results of immuno-EM localization are presented in quantitative form in Table II. Evaluation of reductase expression in the ER was done with a calibrated grid on cytoplasmic areas not containing mitochondria. Grid cells were defined as PDI positive or negative, according to their content of 10-nm gold particles (see Materials and Methods). As can be seen from the third and fifth columns of Table II, reductase labeling was nearly three times higher in PDI-positive areas than in PDI-negative ones, and the extent of labeling was similar for wt and G2A cells in this experiment. In contrast, in wt cells the extent of labeling of mitochondria was >10-fold higher than that of G2A cells, where the density of 5-nm gold particles over mitochondria was similar to that found in the nonmito-

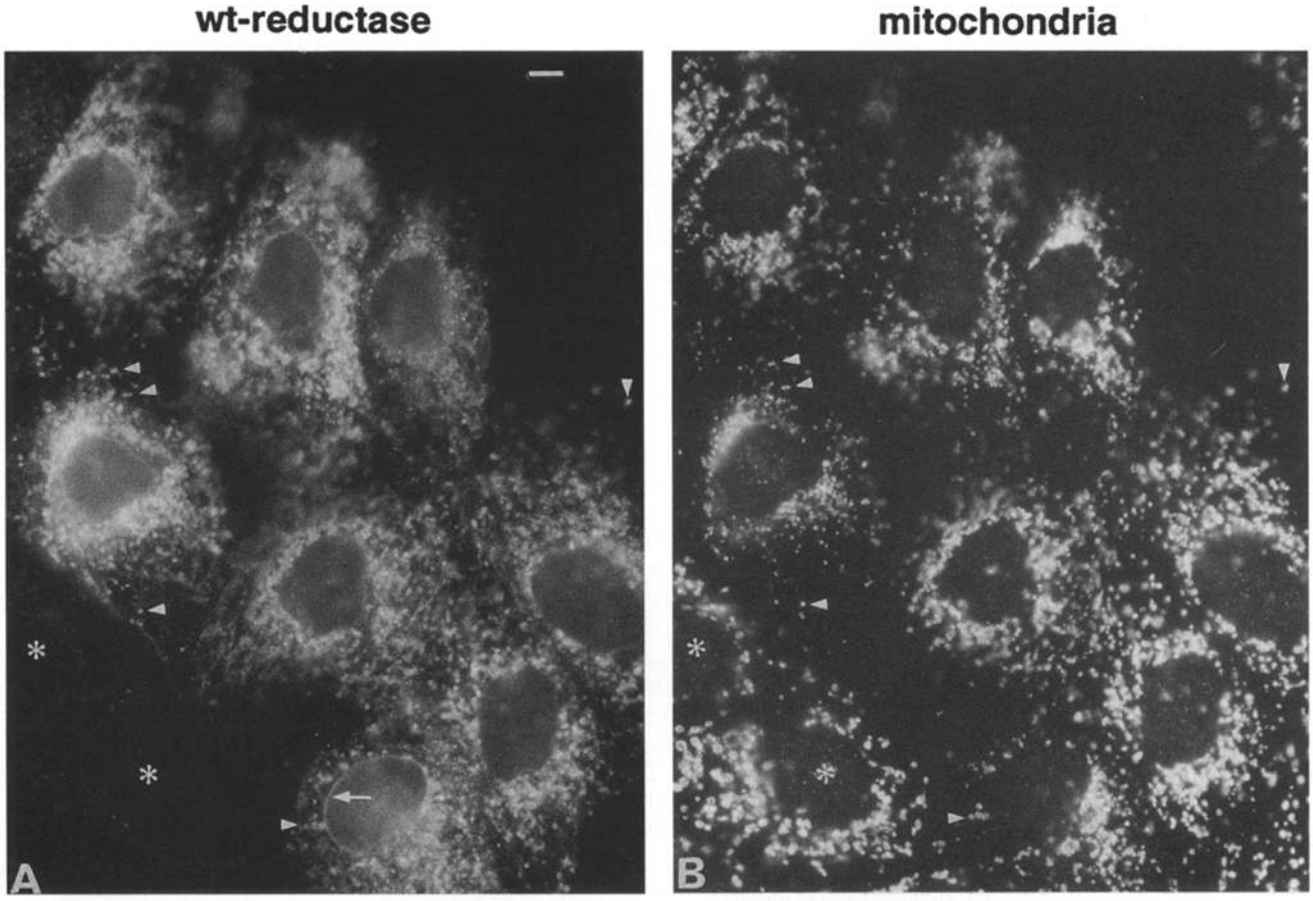

Figure 3. Double-staining immunofluorescence of wt-MDCK cells: comparison between localization of reductase and mitochondria. Cells expressing wt-reductase were doubly stained with a goat polyclonal antibody against rat cyt b_5 reductase and a rabbit polyclonal antibody against bovine complex III. Reductase and complex III were revealed with biotinylated monoclonal anti–goat IgG, followed by Texas red–conjugated streptavidin (*A*) and FITC-conjugated donkey anti–rabbit IgG (*B*), respectively. The figure shows the same field of cells viewed under the rhodamine (*A*) or FITC (*B*) filter. Reductase (*A*) shows a punctate pattern superimposed on a more diffuse reticular stain. The punctate pattern is in great part coincident with the pattern obtained with the anti–complex III antibody. Arrowheads in *A* and *B* indicate some of the points of coincidence. In addition, the anti-reductase antibody clearly stains the nuclear envelope (*A*, *arrow*), which is not stained by the anti–complex III antibody (*B*). Asterisks in both panels indicate cells that express low levels of reductase. Bar, 5 μm.

chondrial PDI-negative areas (Table II, *seventh column*). The same result was obtained when the linear density of gold particles per contour length of mitochondrial profiles was calculated (*ninth column*). Thus, with similar levels of labeling of the ER, the G2A-expressing cells showed dramatically reduced levels of mitochondrial labeling, indicating that lack of myristoylation interferes with MOM localization of the reductase. It should be mentioned that the data of Table II cannot be used to directly compare labeling density in the ER with that in mitochondria, since the grid method used to define PDI-positive and -negative areas results in the inclusion of cytoplasm surrounding ER cisternae in the total areas used to calculate gold particle density.

Comparison of Localization of wt and G2A Reductase by Cell Fractionation

To obtain further quantitative evaluation of the different subcellular distribution of the two reductase forms, cell fractions from wt- and G2A-MDCK were prepared and analyzed by immunoblotting. A postnuclear supernatant obtained from each cell line was subjected to differential centrifugation to obtain mitochondrial (*Mt*), rapidly sedimenting (heavy) microsomal (*HMR*), microsomal (*MR*), and high speed supernatant (*Sup*) fractions (Fig. 8). Aliquots deriving from the same number of cells were analyzed for a 13-kD polypeptide recognized by the anti–complex III antibody, for ribophorin I as an ER marker, and for reductase (Fig. 8). As can be seen in the lower panel of Fig. 8 *A*, the complex III antibody was almost exclusively recovered in the mitochondrial fraction in both cell lines. In both cell lines, most of the ribophorin I was recovered in the microsomal fraction, but appreciable amounts were found also in the mitochondrial and heavy microsomal fractions (Fig. 8 *A*, *upper panel*). If expressed on a protein basis, the fraction most enriched in ribophorin was the heavy microsomal one. The ribophorin content of the mitochondrial fraction on a protein basis was 30–40% that of the heavy microsomal fraction (see Fig. 10). As can be

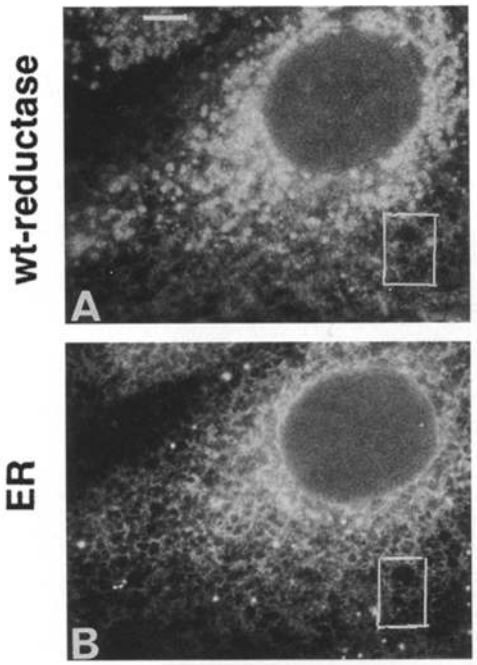

Figure 4. Double-staining immunofluorescence of wt-MDCK cells: comparison between localization of reductase and of ER. Cells expressing wt-reductase were doubly stained with a goat polyclonal antibody against rat cyt b_5 reductase and a rabbit polyclonal antibody against ER membrane proteins. Reductase and ER were revealed with biotinylated monoclonal anti-goat IgG, followed by Texas red–conjugated streptavidin (*A*) and FITC-conjugated donkey anti-rabbit IgG (*B*), respectively. The figure shows the same field of cells viewed under the rhodamine (*A*) or FITC (*B*) filter. Reductase yields the usual punctate plus reticular staining. The reticular staining is coincident with the ER pattern. The boxed area in both panels encloses an area where the coincidence is particularly clear. Bar, 5 μm.

seen from the middle panel of Fig. 8 *A*, the distributions of wt and G2A reductase differed markedly. While the wt enzyme was distributed roughly equally between the mitochondrial and microsomal fractions, the distribution of the G2A mutant was similar to that of ribophorin, suggesting that the presence of the mutant enzyme in the mitochondrial fraction was due to contamination with ER elements. Both wt and G2A reductase were present at nearly undetectable levels in the high speed supernatant. The reductase and ribophorin content was quantitated from blots like the one shown in Fig. 8 *A*, and the ratio of reductase to ribophorin was calculated and normalized to the one found in the microsomal fraction in each experiment. As shown in Fig. 8 *B*, the ratio of wt reductase to ribophorin was over two times higher in the mitochondrial fraction than in the two microsomal fractions, suggesting that >50% of the reductase in the mitochondrial fraction was endogenous to mitochondria and not caused by cross contamination. In contrast, the ratio of reductase to ribophorin for the G2A mutant was the same in mitochondrial and microsomal fractions, indicating that all the reductase recovered in the mitochondrial fraction was contributed by contaminating microsomes. In one experiment, we also determined the reductase content of the fractions with the NADH-$[Fe(CN)_6]^{3-}$ assay, and the ratio of reductase activity to ribophorin (determined by immunoblotting) was calculated and normalized to the ratio found in the microsomal fraction. As shown in Fig. 8 *C*, the result obtained with this procedure agreed well with the data obtained on the basis of immunoblotting.

wt and G2A Reductase Both Behave as Integral Membrane Proteins

Although G2A reductase was associated with ER membranes on the basis of both morphological and cell fractionation experiments, it was possible that, because of the absence of myristic acid, it was only weakly associated with the phospholipid bilayer. To investigate a possible role of myristic acid in strengthening the association between reductase and membranes, we treated a total membrane fraction from wt- and G2A-MDCK cells with agents routinely used to discriminate between integral and peripheral membrane proteins (Fig. 9). Both wt and G2A reductase were resistant to extraction with Na_2CO_3, pH 11.2 (Fig. 9, lanes *1-4*), and both were recovered exclusively in the detergent phase after extraction with Triton X-114 (Fig. 9, lanes *5-8*). Thus, by both these criteria, wt and G2A reductase were indistinguishable and behaved like integral membrane proteins.

Pulse-Chase Analysis of Targeting of wt and G2A Reductase

The absence of G2A reductase from mitochondria could be explained either by a failure of the newly synthesized mutant to bind to the MOM or by a high degree of instability of the enzyme on the MOM but not on ER membranes. In the latter case, after binding to the MOM, it would be rapidly degraded, resulting in a low, undetectable, steady state reductase concentration on that membrane. To distinguish between these two possibilities, we carried out a pulse-chase experiment in which we analyzed the degree of metabolic labeling in the mitochondrial and heavy microsomal fraction of wt and G2A reductase after various times of chase (Fig. 10). We normalized the amount of metabolic labeling to the amount of total reductase in each immunoprecipitate (see Materials and Methods). In this way, we corrected for differences in reductase recovery in the immunoprecipitates (caused by the low [~50%] efficiency of immunoprecipitation of our antibodies). Moreover, this method permitted direct comparison of the extent of labeling of reductase in the two cell fractions, independent of its concentration within the fraction. If the instability hypothesis was the correct one, we expected that G2A reductase in the mitochondrial fraction would show a high degree of metabolic labeling at early time points, with a rapid decrease, caused by degradation, to the level observed in the HMR fraction, when all the labeled reductase immunoprecipitated from the mitochondrial fraction would be due to microsomal contamination. The latter can be estimated by the ratio of ribophorin content of the two fractions, and it is given in the lower line of Fig. 10. As can be seen from Fig. 10, the extent of labeling of both wt and G2A reductase did not change significantly in either cell fraction during nearly 4 h of chase, indicating that both forms of reductase were stable. Moreover, the metabolic specific radioactivity of G2A reductase in the

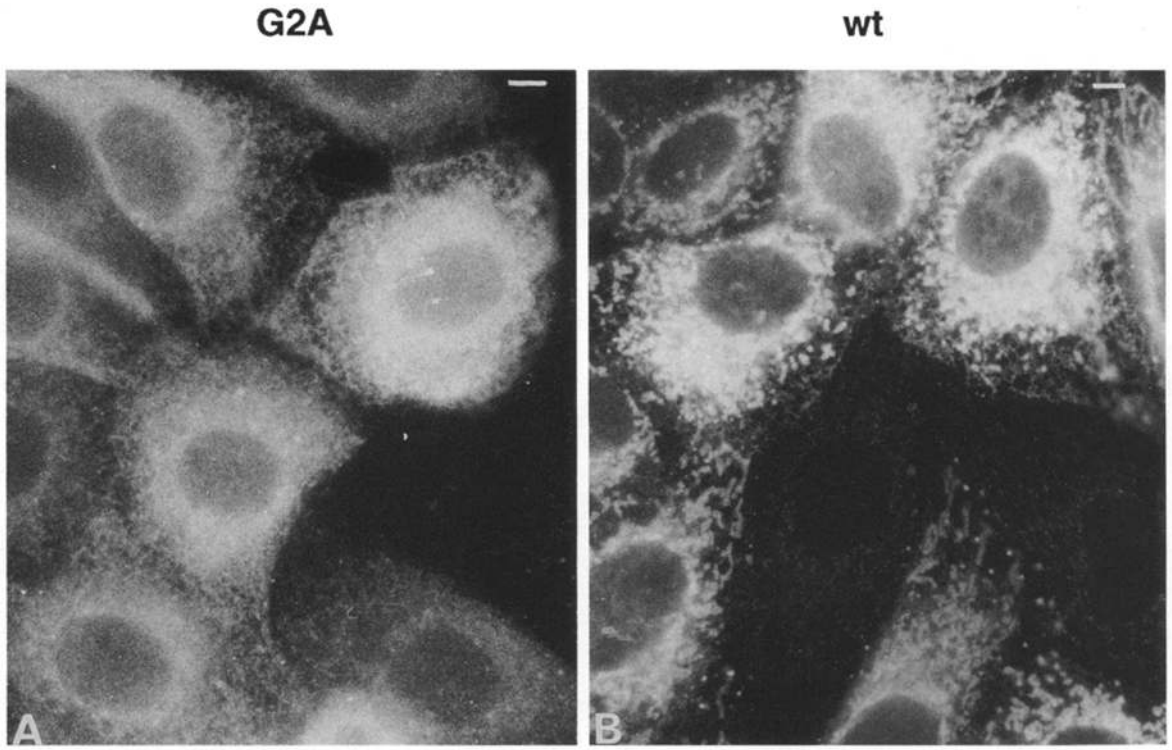

Figure 5. Comparison of wt and G2A localization in stably expressing MDCK cells. G2A- (*A*) and wt- (*B*) MDCK were immunostained with a polyclonal rabbit anti–rat reductase antibody, which was revealed by biotinylated goat anti–rabbit IgG, followed by Texas red–conjugated streptavidin. wt reductase shows the expected punctate (mitochondria) plus reticular (ER) staining. In two cells in the lower part of the field of *B*, mitochondria appear as elongated bodies. Their appearance as dots or more elongated bodies depends on their orientation with respect to the monolayer. In G2A reductase–expressing cells (*A*), the antibody does not stain any discrete structures reminiscent of mitochondria, but it yields only the diffuse reticular staining characteristic of the ER. Bar, 5 μm.

mitochondrial fraction was not significantly different from the value found for the mutant in the heavy microsomal fraction (Fig. 10, *right*), as would be expected if the metabolically labeled G2A reductase recovered in the mitochondrial fraction is nearly exclusively due to contaminating microsomes. The results of this experiment are thus consistent with the hypothesis that G2A reductase fails to associate with the MOM. The alternative, unlikely interpretation is that it does associate but is degraded within the 5-min pulse period of the experiment.

Discussion

Although N-myristoylation by itself is not sufficient to anchor proteins to the phospholipid bilayer (Peitzsch and McLaughlin, 1993), it can collaborate with other features of modified proteins to ensure docking to the cytoplasmic face of a variety of membranes. For *src* and myristoylated alanine-rich protein kinase C substrate, basic residues near the NH_2 terminus, which interact with acidic phospholipids, are required, in addition to myristic acid for association with membranes (Sigal et al., 1994; Taniguchi and Manenti, 1993). In other proteins like *arf* or recoverin, myristic acid is part of a switch mechanism, permitting membrane association when a ligand such as GTP or Ca^{2+} occupies a binding site elsewhere within the polypeptide (Randazzo et al., 1995; Zozulya and Stryer, 1992). In no myristoylated protein, however, has a role for myristic acid in the selection of the target membrane been demonstrated. In the present study, we have chosen NADH-cytochrome b_5 reductase as model protein to address the question of the role of myristic acid in targeting. Since a hydrophobic stretch of amino acids slightly downstream to the NH_2 terminus interacts with the phospholipid bilayer (Kensil and Strittmatter, 1986), this enzyme has offered us the possibility to investigate the targeting role of N-myristoylation independently from its anchoring function.

One Protein Is Targeted to Two Compartments by Two Different Mechanisms

Studies on man (Katsube et al., 1991; Shirabe et al., 1994) and rat (Pietrini et al., 1992, 1988) indicate that NADH-cyt b_5 reductase is encoded in one gene, which generates both the soluble, erythrocyte-specific form and the ubiquitously expressed, myristoylated forms. The latter is docked to membranes via an NH_2-terminal anchor, containing 14 uncharged residues, and exposes its COOH-terminal catalytic domain to the cytosol (for review see Borgese et al., 1993). In man, a point mutation causing the complete absence of immunologically measurable reductase resulted in the absence of both ER and MOM reductase enzyme activity in cultured fibroblasts, demonstrating that the same gene product is localized to two different compartments (Shirabe et al., 1995). Previous biochemical studies had indicated that the same reductase molecule is present

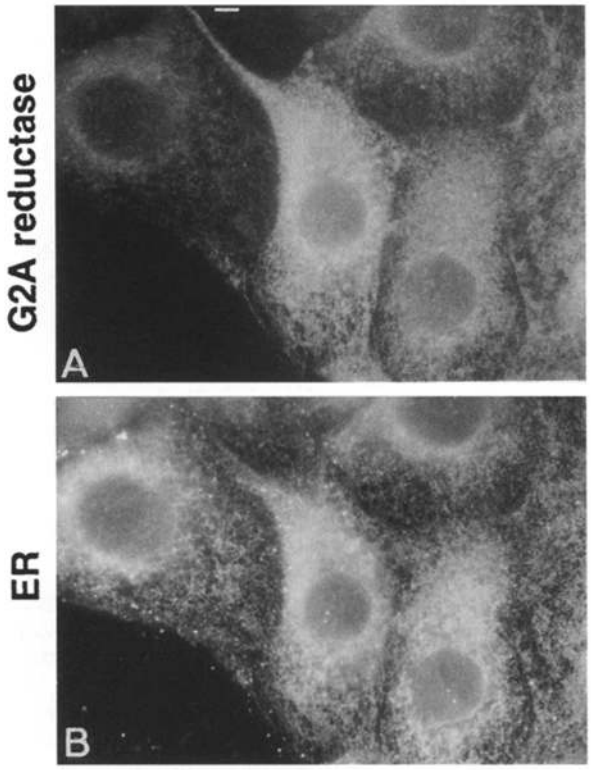

Figure 6. Double-staining immunofluorescence of MDCK cells expressing G2A reductase reveals only an ER localization for the mutant reductase. G2A-MDCK cells were doubly immunostained with anti-reductase (*A*) and anti-ER antibodies (*B*), as explained in the legend to Fig. 4. An essentially identical pattern is obtained with the two antibodies in all cells. Bar, 5 μm.

on these two membranes (for review see Borgese et al., 1993), predicting that both would be myristoylated, as directly demonstrated in a subsequent study (Borgese and Longhi, 1990). The present work, which shows that the product of one cDNA, coding for cyt b_5 reductase, localizes both to mitochondria and to the ER, confirms and strengthens the conclusion that the same protein is targeted to two biogenetically independent membranes. However, the results of this paper also indicate that the mechanism of targeting of reductase to these two membranes is different, since localization to the MOM, but not to the ER membrane, requires the presence of N-linked myristic acid. This was demonstrated by comparing the localization of the wt and a nonmyristoylatable G2A mutant of reductase in transfected mammalian cells by immunofluorescence, immuno-EM, and cell fractionation. Pulse-chase experiments suggested that the G2A mutant lost its capacity to target to the MOM, while it retained the ability to specifically associate with the ER membrane, presumably via the stretch of 14 uncharged residues close to the NH_2 terminus. In its ER location, the mutant, like the wt reductase, behaved like an integral membrane protein on the basis of its resistance to extraction by alkali and its partition into the detergent phase after treatment with Triton X-114. Thus, in agreement with a previous in vitro study (Strittmatter et al., 1993), our results show that, also in vivo, N-myristoylation is not required for anchoring of reductase to the phospholipid bilayer, and, in addition, reveal a novel role for the NH_2-terminal myristoylated glycine in protein targeting.

It is interesting that the yeast homologue of mammalian cyt b_5 reductase is not myristoylated, but it also contains targeting information for the MOM at its NH_2 terminus (Hahne et al., 1994). The yeast reductase is partly anchored to the MOM, with the cytosolic COOH-terminal catalytic domain exposed to the cytosol as in mammals,

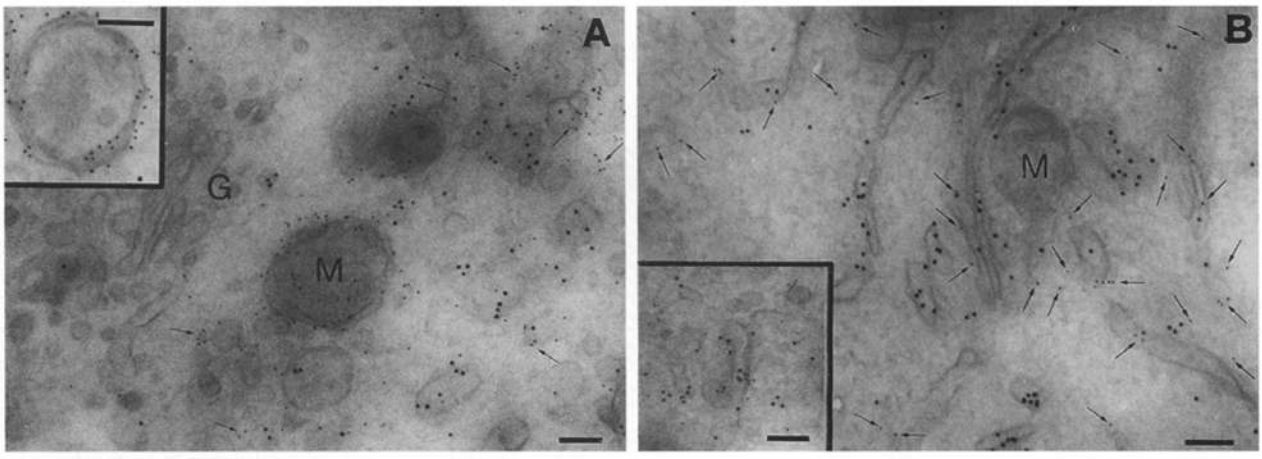

Figure 7. Immunogold-EM localization of wt and G2A-reductase in stably expressing MDCK cells. Ultrathin cryosections obtained from wt (*A*) or G2A (*B*) reductase–expressing cells were incubated with anti-PDI antibodies followed by secondary antibody–10-nm gold particle conjugates, and then with anti-reductase antibodies followed by secondary antibody–5-nm gold particle conjugates. wt reductase is seen both at the periphery of mitochondria (*M*, *inset*) and on PDI-positive structures. The Golgi Complex (*G*) is negative. (*A*, *inset*) Mitochondrion at slightly higher magnification, to illustrate how the labeling is mainly at the periphery of the organelle. G2A reductase (*B*) is seen on PDI-positive structures but is absent from mitochondria (*M*). (*B*, *inset*) Area where labeling of the ER by anti-PDI and anti-reductase antibodies is particularly evident. Arrows in *A* and *B* point to some of the 5-nm gold particles, indicative of the presence of reductase. Bars: (*A*, *inset*) 0.1 μm; (*B*, *inset*) 0.125 μm.

Table II. Quantitation of Reductase Immunogold Labeling in wt and G2A MDCK Cells

	PDI-positive areas*		PDI-negative areas*		Mitochondria			
	Total area examined	5-nm gold	Total area examined	5-nm gold	Total area examined	5-nm gold	Total contour	5-nm gold
	μm^2	*particles per* $\mu m^2 \pm SEM$	μm^2	*particles per* $\mu m^2 \pm SEM$	μm^2	*particles per* $\mu m^2 \pm SEM$	μm	*particles per* $\mu m \pm SEM$
wt (6)‡	18.7	27.4 ± 2.9	18.5	10.9 ± 0.9	4.4	118.0 ± 11.7	48.1	6.3 ± 0.8
G2A (9)‡	15.6	24.4 ± 3.2	19.7	8.7 ± 1.4	4.7	12.2 ± 4.3	40.3	0.6 ± 0.2

*PDI-positive and -negative areas are the sum of 0.25 × 0.25-μm areas containing more than one gold particle or zero to one gold particles, respectively (see Materials and Methods).
‡Numbers in parentheses refer to number of negatives examined.

cally processed to become a soluble protein of the intermembrane space (Hahne et al., 1994). No soluble reductase has been detected in rat mitochondria; rather, all of it is tightly bound to the MOM (Borgese and Pietrini, 1986) and accessible to antibodies and proteases (Meldolesi et al., 1980). We cannot exclude, however, that a small fraction of MOM-anchored mammalian reductase has an inverted topology, with the catalytic domain facing the intermembrane space so that it can carry out the as yet unknown function of its yeast counterpart.

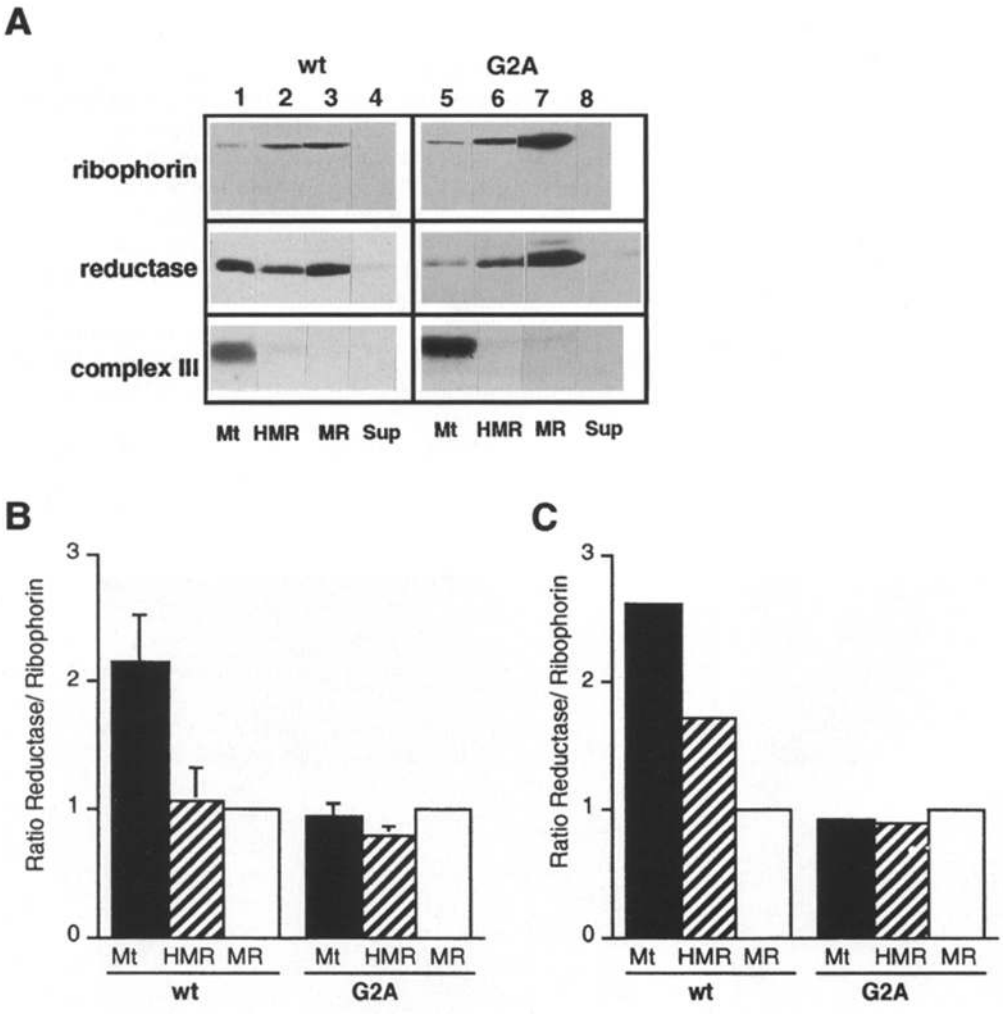

Figure 8. Analysis of cell fractions from wt- and G2A-MDCK cells. (*A*) For each cell line, mitochondrial (*Mt*; lanes *1* and *5*), heavy microsomal (*HMR*; lanes *2* and *6*), microsomal (MR; lanes *3* and *7*), and high speed supernatant (*sup*; lanes *4* and *8*) fractions were prepared by differential centrifugation from cells grown to ~70% confluency on 175 cm^2 petri dishes (see Materials and Methods). Equal aliquots of the cell fractions, corresponding to 5% of the total recovered material, were analyzed by 11% SDS-PAGE, followed by blotting onto nitrocellulose. The blots were cut into three strips: the first, from the origin to the 50,000-M_r position; the second, encompassing the region between 50 and 21,000 kD; and the third, from the 21,000-M_r position to the front. The three regions (from top to bottom) were probed respectively with anti-ribophorin, anti-reductase, and anti–complex III antibodies. The latter recognized all the polypeptides of the complex (see Materials and Methods), but the polypeptide with apparent M_r ~13,000 was chosen because of its convenient position on the gel. Bands were revealed by ECL. (*B*) Ratio of reductase to ribophorin determined by immunoblotting in cell fractions normalized to that ratio found in the MR fraction. Cell fractions from wt- (*left*) and G2A- (*right*) MDCK were analyzed as in *A*, but using ^{125}I–protein A as secondary reagent. The autoradiograms were scanned, and the areas corresponding to the ribophorin and reductase bands were determined. The results are averages of three separate experiments ± SEM. Filled, striped, and open bars represent mitochondrial, heavy microsomal, and microsomal fractions, respectively. (*C*) Ratio of reductase enzyme activity to ribophorin (determined by immunoblotting) in cell fractions. Reductase concentration, determined by the NADH-$[Fe(CN)_6]^{3-}$ reductase activity, was divided by the ribophorin concentration (peak area per μl of cell fraction). The values obtained were normalized to that of the same ratio found in the MR fraction. Values refer to one experiment. Bars, as in *B*.

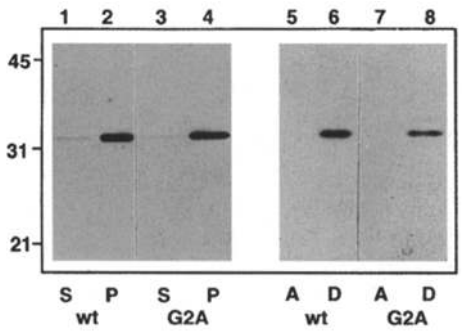

Figure 9. wt and G2A reductase both behave as integral membrane proteins. A total membrane fraction obtained from wt- (lanes *1*, *2*, *5*, and *6*) or G2A- (lanes *3*, *4*, *7*, and *8*) MDCK was treated with 0.1 M Na_2CO_3, pH 11.2 (lanes *1–4*), or Triton X-114 (lanes *5–8*). After Na_2CO_3 treatment, the samples were centrifuged to obtain pellet (*P*) and supernatant (*S*) fractions. After Triton X-114 extraction, the detergent (*D*) and aqueous (*A*) phases were separated. Equal aliquots of *P*, *S*, *D*, and *A* fractions were analyzed by SDS-PAGE followed by ECL immunoblotting with anti-reductase antibodies. Numbers on the left indicate $M_r \times 10^{-3}$ of molecular weight standards.

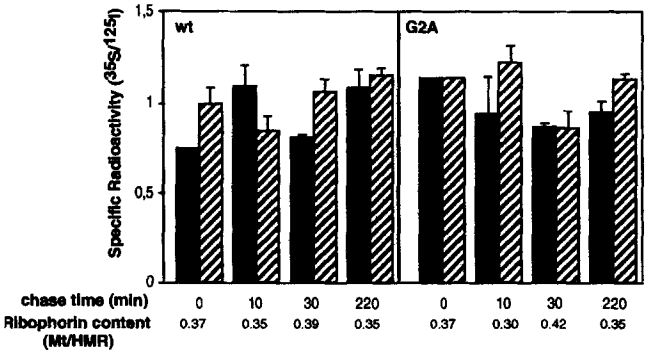

Figure 10. Targeting of wt- and G2A-reductase analyzed in a pulse-chase experiment. wt- (*left*) or G2A- (*right*) MDCK cells were pulse labeled with [^{35}S]methionine + cysteine (0.4 mCi/ml final concentration) for 5 min, and then incubated in complete medium for the indicated chase times. Mitochondrial (*Mt*; *filled bars*) and heavy microsomal (*HMR*; *striped bars*) fractions were prepared, and the ribophorin content (peak area by radioimmunoblotting per mg protein) was determined. The ratio of the ribophorin content in Mt to that in HMR is indicated on the bottom line of the figure. Reductase was immunoprecipitated from the fractions, and metabolic specific radioactivity (ratio of ^{35}S-labeled molecules to total molecules detected by radioimmunoblotting with ^{125}I–protein A; see Materials and Methods) was determined. The results shown are averages of values obtained with two separate immunoprecipitates ± half range.

What Is the Role of Myristic Acid in Targeting cyt b_5 Reductase to the MOM?

At present, the structural characteristics of MOM proteins required for their targeting have not been identified. The targeting sequence(s) is in no case cleaved after insertion into the MOM, as occurs for most proteins directed to internal mitochondrial subcompartments (for review see Shore et al., 1995). While in a few cases a positively charged sequence resembling a matrix-directing signal, followed by a hydrophobic stretch, seemed to constitute the targeting signal (Hurt et al., 1985; Hahne et al., 1994), the putative matrix-directing signal has not been found on most MOM proteins, and on one protein on which it is present (mas70p), it was found to be dispensable for targeting (McBride et al., 1992). The targeting information for the MOM often seems to be close to or to coincide with the membrane-anchoring region; i.e., it is located at the COOH terminus in proteins anchored by a COOH terminal tail (De Silvestris et al., 1995; Mitoma and Ito, 1992; Cao and Douglas, 1995; Nguyen et al., 1993), and at the NH_2 terminus for proteins with opposite topology (McBride et al., 1992).

Current evidence supports the idea that proteins destined for the MOM follow the initial steps of the import pathway taken by matrix-directed protein precursors (Shore et al., 1995; Kiebler et al., 1993). It is thought that MOM proteins, after binding to import receptors on the mitochondrial surface, somehow abandon the import pathway at an early stage, remaining inserted in the outer membrane. The picture is complicated by the finding that mitochondria have multiple import receptors, which have different specificities and may act cooperatively (Haucke et al., 1995). Thus, different structural features on different proteins could account for targeting to the MOM. In addition, cytosolic factors that assist import of matrix-directed precursors (Hachiya et al., 1993; Murakami et al., 1992) may also participate in targeting of MOM proteins.

With this information in mind, what mechanism can be proposed for the role of N-linked myristic acid in targeting of cyt b_5 reductase to the MOM? At present, we do not have the means to determine whether wt myristoylated reductase follows the insertion pathway used by other MOM proteins because we have been unable to establish an in vitro system reflecting the in vivo targeting specificity. Although in vitro–synthesized reductase does bind to membranes in a Na_2CO_3-resistant fashion (Pietrini et al., 1992), we have not been able to demonstrate specificity in the choice of a membrane, nor a temperature or energy requirement (unpublished results). Factors operating in vivo, which limit the nonspecific binding of reductase to phospholipid bilayers, could be absent from the in vitro system. In addition, efficiency of myristoylation in the cell-free system might be low.

Whether or not reductase uses a general import pathway for MOM insertion, we envision two possible roles for myristic acid in the targeting: (*a*) it could be exposed and be part of the recognition motif that interacts with components of the MOM or with specific soluble import factors and/or chaperones required for MOM targeting; or (*b*) it could have a more indirect role, forcing the NH_2-terminal portion of reductase into a conformation competent for interaction with MOM components or soluble targeting factors. In other proteins, myristic acid has been observed to directly participate in protein–protein interaction, as in the case of picornavirus capsid protein VP4 (Chow et al., 1987), as well as to influence the overall conformation of the acylated protein, as in the case of the Ca^{2+}-free form of recoverin (Tanaka et al., 1995).

Whatever the mechanism by which N-myristoylation affects the targeting of reductase, the observations of this study provide a demonstration of a strikingly specific role of this modification in membrane protein localization. Given the dramatic effect that the presence of myristic

acid has on the choice of the target membrane by reductase, it seems likely that N-myristoylation has a similar role in the targeting also of other proteins.

Targeting to the ER Membrane

The first step in targeting of integral membrane proteins to the ER membrane is generally the cotranslational binding of their NH_2-terminal signal sequence to signal recognition particle (SRP) (for review see Walter and Johnson, 1994). A notable exception to this mechanism is offered by the targeting of so-called tail-anchored proteins, which are integrated in the membrane via a COOH-terminal anchor and expose an NH_2-terminal hydrophilic domain to the cytosol (Kutay et al., 1993). Many tail-anchored proteins are specifically targeted to the ER membrane by an SRP-independent, posttranslational mechanism (Kutay et al., 1993; Borgese et al., 1993). In addition, also some NH_2-terminally "tail-anchored" proteins (NH_2-terminal anchor, COOH-terminal cytosolic domain), such as NADH-cyt b_5 reductase (Borgese and Gaetani, 1980) and the α subunit of SRP receptor (Andrews et al., 1989), become integrated into the ER posttranslationally. In the context of this discussion, we will therefore extend the term "tail-anchored" also to NH_2-terminally anchored proteins.

An open question is how specificity in targeting of tail-anchored proteins is achieved. In the case of synaptobrevin, there is evidence for the involvement of ER proteins (Kutay et al., 1995); on the other hand, insertion of cyt b_5 (not to be confused with cyt b_5 reductase!) appears to be insensitive to pretreatment of the acceptor membranes with proteases (Vergères et al., 1995). If ER proteins are not involved, one might postulate that particular physicochemical characteristics of the ER bilayer make it competent to integrate NH_2- and COOH-terminally tail-anchored proteins. It also is not clear what kind of sequence or structural features tail-anchored proteins must have to be targeted to the ER. One possibility that we favor is that any protein with a hydrophobic stretch close to one of its extremities will insert into the ER membrane, unless it carries a specific signal for another organelle, which would then compete with the ER for the signal-bearing polypeptide. This hypothesis could account for the double localization, on MOM and ER membranes, of some tail-anchored proteins, such as NADH-cyt b_5 reductase (this study and references therein) and bcl-2 (Nguyen et al., 1993). A weak MOM targeting signal could allow a portion of these proteins to escape from the mitochondrial import system and to interact with the less specific ER integration system. This model would also be consistent with the observation of this study that the nonmyristoylated G2A reductase mutant retains its capacity to associate with the ER, while having lost its ability to target to the MOM. While features contributed by N-myristoylation would be required for recognition by the more specific mitochondrial import machinery, the hydrophobic stretch near the NH_2 terminus would be sufficient for interaction with the more permissive ER integration system.

We thank Mr. Franco Crippa for technical assistance in electron microscopy, and Drs. Kathryn Howell and Emanuela Pedrazzini for critically reading the manuscript.

This work was partially supported by Consiglio Nazionale delle Ricerche grants CT94.02558.CT04 and "Progetto finalizzato Ingegneria Genetica," and by Telethon grant E081, awarded to N. Borgese.

Received for publication 2 April 1996 and in revised form 16 September 1996.

References

Aitken, A., P. Cohen, S. Santikarn, D.H. Williams, A.G. Calder, A. Smith, and C.B. Klee. 1982. Identification of the NH_2-terminal blocking group of calcineurin B as myristic acid. *FEBS Lett.* 150:314–318.

Ames, J.B., T. Porumb, T. Tanaka, M. Ikura, and L. Stryer. 1995. Amino-terminal myristoylation induces cooperative calcium binding to recoverin. *J. Biol. Chem.* 270:4526–4533.

Andrews, D.W., L. Lauffer, P. Walter, and V.R. Lingappa. 1989. Evidence for a two-step mechanism involved in assembly of functional signal recognition particle receptor. *J. Cell Biol.* 108:797–810.

Ausubel, F.M., R. Brent, R.E. Kingston, D.D. Moore, J.G. Seidman, J.A. Smith, and K. Struhl. 1987. Current Protocols in Molecular Biology. John Wiley and Sons, Inc.

Bassetti, M., D. Lodi Pasini, and P. Rosa. 1995. Degradation of gonadotropin β-subunits retained in the endoplasmic reticulum of the gonadotropes of castrated rats. *Endocrinology.* 136:1168–1176.

Bonner, W.M., and R.A. Laskey. 1974. A film detection method for tritium-labelled proteins and nucleic acids in polyacrylamide gels. *Eur. J. Biochem.* 46:83–88.

Bordier, C. 1981. Phase separation of integral membrane proteins in Triton X-114 solution. *J. Biol. Chem.* 256:1604–1607.

Borgese, N., and S. Gaetani. 1980. Site of synthesis of rat liver NADH-cytochrome b_5 reductase, an integral membrane protein. *FEBS Lett.* 112:216–220.

Borgese, N., and R. Longhi. 1990. Both the outer mitochondrial membrane and the microsomal forms of cytochrome b_5 reductase contain covalently bound myristic acid. Quantitative analysis on the polyvinylidene difluoride-immobilized proteins. *Biochem. J.* 266:341–347.

Borgese, N., and G. Pietrini. 1986. Distribution of the integral membrane protein NADH-cytochrome b_5 reductase in rat liver cells, studied with a quantitative radioimmunoblotting assay. *Biochem. J.* 239:393–403.

Borgese, N., G. Pietrini, and J. Meldolesi. 1980. Localization and biosynthesis of NADH-cytochrome b_5 reductase, an integral membrane protein, in rat liver cells. III. Evidence for the independent insertion and turnover of the enzyme in various subcellular compartments. *J. Cell Biol.* 86:38–45.

Borgese, N., A. D'Arrigo, M. De Silvestris, and G. Pietrini. 1993. NADH-cytochrome b_5 reductase and cytochrome b_5: the problem of postranslational targeting to the endoplasmic reticulum. *In* Subcellular Biochemistry. Vol. 21. N. Borgese and J.R. Harris, editors. Plenum Press, New York. 313–341.

Brewer, C.B., and M.G. Roth. 1991. A single amino acid change in the cytoplasmic domain alters the polarized delivery of influenza virus hemagglutinin. *J. Cell Biol.* 114:413–421.

Busconi, L., and T. Michel. 1993. Endothelial nitric oxide synthase. N-terminal myristoylation determines subcellular localization. *J. Biol. Chem.* 268:8410–8413.

Cao, W., and M.G. Douglas. 1995. Biogenesis of ISP6, a small carboxyl-terminal anchored protein of the receptor complex of the mitochondrial outer membrane. *J. Biol. Chem.* 270:5674–5679.

Carr, S.A., K. Biemann, S. Shoji, D.C. Parmelee, and K. Titani. 1982. *n*-tetradecanoyl is the NH_2-terminal blocking group of the catalytic subunit of cyclic AMP-dependent protein kinase from bovine cardiac muscle. *Proc. Natl. Acad. Sci. USA.* 79:6128–6131.

Casey, P.J. 1995. Protein lipidation in cell signaling. *Science (Wash. DC).* 268: 221–225.

Cham, B.E., and B.R. Knowles. 1976. A solvent system for delipidation of plasma or serum without protein precipitation. *J. Lipid Res.* 17:176–181.

Chow, M., J.F.E. Newman, D. Filman, J.M. Hogle, D.J. Rowlands, and F. Brown. 1987. Myristoylation of picornavirus capsid protein VP4 and its structural significance. *Nature (Lond.).* 327:482–486.

Cross, F.R., E.A. Garber, D. Pellman, and H. Hanafusa. 1984. A short sequence in the p60src N terminus is required for p60src myristoylation and membrane association and for cell transformation. *Mol. Cell. Biol.* 4:1834–1842.

D'Souza-Schorey, C., and P.D. Stahl. 1995. Myristoylation is required for the intracellular localization and endocytic function of ARF6. *Exp. Cell Res.* 221:153–159.

De Silvestris, M., A. D'Arrigo, and N. Borgese. 1995. The targeting information of the mitochondrial outer membrane isoform of cytochrome b_5 is contained within the carboxyl-terminal region. *FEBS Lett.* 370:69–74.

Franco, M., P. Chardin, M. Chabre, and S. Paris. 1995. Myristoylation of ADP-ribosylation factor 1 facilitates nucleotide exchange at physiological Mg^{2+} levels. *J. Biol. Chem.* 270:1337–1341.

Graff, J.M., J.I. Gordon, and P.J. Blackshear. 1989. Myristoylated and non-myristoylated forms of a protein are phosphorylated by protein kinase C. *Science (Wash. DC).* 1989:503–506.

Graham, F.L., and A.J. Van der Eb. 1973. A new technique for the assay of infectivity of human adenovirus 5 DNA. *Virology.* 52:456–467.

Hachiya, N., R. Alam, Y. Sakasegawa, K. Mihara, and T. Omura. 1993. A mito-

chondrial import factor purified from rat liver cytosol is an ATP-dependent conformational modulator for precursor proteins. *EMBO (Eur. Mol. Biol. Organ.) J.* 12:1579–1586.

Hahne, K., V. Haucke, L. Ramage, and G. Schatz. 1994. Incomplete arrest in the outer membrane sorts NADH-cytochrome b_5 reductase to two different submitochondrial compartments. *Cell.* 79:829–839.

Harris, M.P.G., and J.C. Neil. 1994. Myristoylation-dependent binding of HIV-1 Nef to CD4. *J. Mol. Biol.* 241:136–142.

Haucke, V., T. Lithgow, S. Rospert, K. Hahne, and G. Schatz. 1995. The yeast mitochondrial protein import receptor Mas20p binds precursor proteins through electrostatic interaction with the positively charged presequence. *J. Biol. Chem.* 270:5565–5570.

Hurt, E.C., U. Müller, and G. Schatz. 1985. The first twelve amino acids of a yeast mitochondrial outer membrane protein can direct a nuclear-coded cytochrome oxidase subunit to the mitochondrial inner membrane. *EMBO (Eur. Mol. Biol. Organ.) J.* 4:3509–3518.

Johnson, D.R., R.S. Bhatnager, L.J. Knoll, and J.I. Gordon. 1994. Genetic and biochemical studies of protein N-myristoylation. *Annu. Rev. Biochem.* 63: 869–914.

Jones, T.L.Z., W.F. Simonds, J.J. Merendino, M.R. Brann, and A.M. Spiegel. 1990. Myristoylation of an inhibitory GTP-binding protein α subunit is essential for its membrane attachment. *Proc. Natl. Acad. Sci. USA.* 87:568–572.

Katsube, T., N. Sakamoto, Y. Kobayashi, R. Seki, M. Hirano, K. Tanishima, A. Tomoda, E. Takazakura, T. Yubisui, M. Takeshita et al. 1991. *Am. J. Hum. Genet.* 48:799–808.

Kensil, C.R., and P. Strittmatter. 1986. Binding and fluorescence properties of the membrane domain of NADH-cytochrome b_5 reductase. Determination of the depth of trp-16 in the bilayer. *J. Biol. Chem.* 261:7316–7321.

Kiebler, M., K. Becker, N. Pfanner, and W. Neupert. 1993. Mitochondrial protein import: specific recognition and membrane translocation of preproteins. *J. Membr. Biol.* 135:191–207.

Kutay, U., E. Hartmann, and T.A. Rapoport. 1993. A class of membrane proteins with C-terminal anchor. *Trends Cell Biol.* 3:72–75.

Kutay, U., G. Ahnert-Hilgen, E. Hartmann, B. Wiedenmann, and T.A. Rapoport. 1995. Transport route for synaptobrevin via a novel pathway of insertion into the endoplasmic reticulum membrane. *EMBO (Eur. Mol. Biol. Organ.) J.* 14:224–231.

Linder, M.E., I.-H. Pang, R.J. Duronio, J.I. Gordon, P.C. Sternweis, and A.G. Gilman. 1991. Lipid modifications of G protein subunits. Myristoylation of $G_o\alpha$ increases its affinity for $\beta\gamma$. *J. Biol. Chem.* 266:4654–4659.

Louvard, D., H. Reggio, and G. Warren. 1982. Antibodies to the Golgi complex and the rough endoplasmic reticulum. *J. Cell Biol.* 92:92–107.

Lowry, O.H., N.J. Rosebrough, A.L. Farr, and R.J. Randall. 1951. Protein measurement with the Folin phenol reagent. *J. Biol. Chem.* 193:265–275.

McBride, H.M., D.G. Millar, J.-M. Li, and G.C. Shore. 1992. A signal-anchor sequence selective for the mitochondrial outer membrane. *J. Cell Biol.* 119: 1451–1456.

McLaughlin, S., and A. Aderem. 1995. The myristoyl-electrostatic switch: a modulator of reversible protein-membrane interactions. *Trends Biochem. Sci.* 20:272–276.

Meldolesi, J., G. Corte, G. Pietrini, and N. Borgese. 1980. Localization and biosynthesis of NADH-cytochrome b_5 reductase, an integral membrane protein, in rat liver cells. II. Evidence that a single enzyme accounts for the activity in its various subcellular locations. *J. Cell Biol.* 85:516–526.

Mitoma, J.-Y., and A. Ito. 1992. Mitochondrial targeting signal of rat liver monoamine oxidase B is located at its carboxy terminus. *J. Biochem.* 111:20–24.

Mumby, S.M., R.O. Heukeroth, J.I. Gordon, and A.G. Gilman. 1990. G-protein α-subunit expression, myristoylation, and membrane association in COS cells. *Proc. Natl. Acad. Sci. USA.* 87:728–732.

Murakami, K., S. Tanase, Y. Morino, and M. Mori. 1992. Presequence binding factor-dependent and -independent import of proteins into mitochondria. *J. Biol. Chem.* 267:13119–13122.

Nguyen, M., D.G. Millar, V.W. Yong, S.J. Korsmeyer, and G.C. Shore. 1993. Targeting of Bcl-2 to the mitochondrial outer membrane by a COOH-terminal signal anchor sequence. *J. Biol. Chem.* 268:25265–25268.

Nicchitta, C.V., G. Migliaccio, and G. Blobel. 1991. Biochemical fractionation and assembly of the membrane components that mediate nascent chain targeting and translocation. *Cell.* 65:587–598.

Olmsted, J.B. 1981. Affinity purification of antibodies from diazotized paper blots of heterogeneous protein samples. *J. Biol. Chem.* 256:11955–11957.

Ozols, J., S.A. Carr, and P. Strittmatter. 1984. Identification of the NH_2-terminal blocking group of NADH-cytochrome b_5 reductase as myristic acid and the complete amino acid sequence of the membrane-binding domain. *J. Biol. Chem.* 259:13349–13354.

Parker, B.A., and G.R. Stark. 1979. Regulation of simian virus 40 transcription: sensitive analysis of the RNA species present early in infections by virus or viral DNA. *J. Virol.* 31:360–369.

Peitzsch, R.M., and S. McLaughlin. 1993. Binding of acylated peptides and fatty acids to phospholipid vesicles: pertinence to myristoylated proteins. *Biochemistry.* 32:10436–10443.

Pietrini, G., P. Carrera, and N. Borgese. 1988. Two transcripts encode rat cytochrome b_5 reductase. *Proc. Natl. Acad. Sci. USA.* 85:7246–7250.

Pietrini, G., D. Aggujaro, P. Carrera, J. Malisco, A. Vitale, and N. Borgese. 1992. A single mRNA, transcribed from an alternative, erythroid-specific promoter, codes for two nonmyristoylated forms of NADH-cytochrome b_5 reductase. *J. Cell Biol.* 117:975–986.

Randazzo, P.A., T. Terui, S. Sturch, H.M. Fales, A.G. Ferrige, and R.A. Kahn. 1995. The myristylated amino terminus of ADP-ribosylation factor 1 is a phospholipid- and GTP-sensitive switch. *J. Biol. Chem.* 270:14809–14815.

Sambrook, J., E.F. Fritsch, and T. Maniatis. 1989. Molecular Cloning: A Laboratory Manual. Cold Spring Harbor Laboratory, Cold Spring Harbor, NY. 545 pp.

Shirabe, K., Y. Fujimoto, T. Yubisui, and M. Takeshita. 1994. An in-frame deletion of codon 298 of the NADH-cytochrome b_5 reductase gene results in hereditary methemoglobinemia type II (generalized type). A functional implication for the role of the COOH-terminal region of the enzyme. *J. Biol. Chem.* 269:5952–5957.

Shirabe, K., M.T. Landi, M. Takeshita, G. Uziel, E. Fedrizzi, and N. Borgese. 1995. A novel point mutation in a 3′ splice site of the NADH-cytochrome b_5 gene results in immunologically undetectable enzyme and impaired NADH-dependent ascorbate regeneration in cultured fibroblasts of a patient with type II hereditary methemoglobinemia. *Am. J. Hum. Genet.* 57:302–310.

Shore, G.C., H.M. McBride, D.G. Millar, N.A.E. Steenaart, and M. Nguyen. 1995. Import and insertion of proteins into the mitochondrial outer membrane. *Eur. J. Biochem.* 227:9–18.

Sigal, C.T., W. Zhou, C.A. Buser, S. McLaughlin, and M.D. Resh. 1994. Amino-terminal basic residues of Src mediate membrane binding through electrostatic interaction with acidic phospholipids. *Proc. Natl. Acad. Sci. USA.* 91: 12253–12257.

Sottocasa, G.L., B. Kuylenstierna, L. Ernster, and A. Bergstrand. 1967. An electron transport system associated with the outer membrane of liver mitochondria. A biochemical and morphological study. *J. Cell Biol.* 32:415–438.

Strittmatter, P., J.M. Kittler, J.E. Coghill, and J. Ozols. 1993. Interaction of non-myristoylated NADH-cytochrome b_5 reductase with cytochrome b_5-dimyristoylphosphatidylcholine vesicles. *J. Biol. Chem.* 268:23168–23171.

Tanaka, T., J.B. Ames, T.S. Harvey, L. Stryer, and M. Ikura. 1995. Sequestration of the membrane-targeting myristoyl group of recoverin in the calcium-free state. *Nature (Lond.).* 376:444–447.

Taniguchi, H., and S. Manenti. 1993. Interaction of myristoylated alanine-rich protein kinase C substrate (MARCKS) with membrane phospholipids. *J. Biol. Chem.* 268:9960–9963.

Vaitukaitis, J.L. 1981. Production of antisera with small doses of immunogen: multiple intradermal injections. *Methods Enzymol.* 73:46–52.

Vergères, G., J. Ramsden, and L. Waskell. 1995. The carboxyl terminus of the membrane-binding domain of cytochrome b_5 spans the bilayer of the endoplasmic reticulum. *J. Biol. Chem.* 270:3414–3422.

Walter, P., and A.E. Johnson. 1994. Signal sequence recognition and protein targeting to the endoplasmic reticulum membrane. *Annu. Rev. Cell Biol.* 10: 87–120.

Yonemoto, W., M.L. McGlone, and S.S. Taylor. 1993. N-myristoylation of the catalytic subunit of cAMP-dependent protein kinase conveys structural stability. *J. Biol. Chem.* 268:2348–2352.

Yu, C.A., L. Yu, and T.E. King. 1974. Soluble cytochrome b-c_1 complex and the reconstitution of succinate-cytochrome c reductase. *J. Biol. Chem.* 249:4905–4910.

Yu, G., and R.L. Felsted. 1992. Effect of myristoylation on p27 nef subcellular distribution and suppression of HIV-LTR transcription. *Virology.* 187:46–55.

Zhu, D., M.E. Cardenas, and J. Heitman. 1995. Myristoylation of calcineurin B is not required for function or interaction with immunophilin-immunosuppressant complexes in the yeast *Saccharomyces cerevisiae*. *J. Biol. Chem.* 270:24831–24838.

Zozulya, S., and L. Stryer. 1992. Calcium-myristoyl protein switch. *Proc. Natl. Acad. Sci. USA.* 89:11569–11573.